Structural Analysis of Bioengineered α-D-Glucan Produced by a Triple Mutant of the Glucansucrase GTF180 Enzyme from *Lactobacillus reuteri* Strain 180: Generation of (α1→4) Linkages in a Native (1→3)(1→6)-α-D-Glucan

Sander S. van Leeuwen,[†] Slavko Kralj,[‡,§] Gerrit J. Gerwig,[†] Lubbert Dijkhuizen,[‡,§] and Johannis P. Kamerling*[,†]

Department of Bio-Organic Chemistry, Bijvoet Center, Utrecht University, 3584 CH Utrecht, The Netherlands, Department of Microbiology, Groningen Biomolecular Sciences and Biotechnology Institute, University of Groningen, 9751 NN Haren, The Netherlands, and Centre for Carbohydrate Bioprocessing, TNO - University of Groningen, 9750 AA Haren, The Netherlands

Received April 16, 2008; Revised Manuscript Received May 15, 2008

Site-directed mutagenesis of the glucansucrase *gtf180* gene from *Lactobacillus reuteri* strain 180 was used to transform the active site region. The α-D-glucan (**mEPS-PNNS**) produced by the triple mutant V1027P:S1137N:A1139S differed in structure from that of the wild-type α-D-glucan (**EPS180**). Besides (α1→3) and (α1→6) linkages, as present in **EPS180**, **mEPS-PNNS** also contained (α1→4) linkages. Linkage analysis, periodate oxidation, and 1D/2D ^{1}H NMR spectroscopy of the intact **mEPS-PNNS**, as well as MS and NMR analysis of oligosaccharides obtained by partial acid hydrolysis of **mEPS-PNNS** afforded a composite model, which includes all identified structural features.

Introduction

Lactic acid bacteria (LAB), like *Lactobacilli*, excrete exopolysaccharides (EPSs) into their surroundings. Exopolysaccharides have been found as adhesives,[1] participants in certain cellular recognition processes,[2] and as slime forming agents for protection against dehydration, phagocytosis, or toxins.[2] The physical properties that are important for their in vivo functions also make these polysaccharides suitable for the food and dairy industry. Bacterial exopolysaccharides have been used as thickeners, stabilizers, and gelling agents.[3] To improve these properties, attention has been paid to the engineering of polysaccharide structures via chemical[4] or enzymatic derivatizations[5–7] and by genetic modification of source micro-organisms.[8,9]

Recently, a family of glucansucrases was discovered in *Lactobacillus reuteri*, which converts sucrose into large, heavily branched α-D-glucans. Structural analysis of the homopolysaccharides produced by the glucansucrases GTF180 and GTFA revealed highly complex structures, and composite models have been proposed.[10,11] Previous studies on the site-directed mutagenesis near the catalytic Asp1133 (putative transition state stabilizing residue) of GTFA have shown that specific amino acid mutations in this glucansucrase gave rise to large changes in the EPS structure and its properties.[12] Similar modifications in the homologous region of the *gtf180* gene have been performed (unpublished data). The EPS of the triple mutant V1027P:S1137N:A1139S (**mEPS-PNNS**) showed the most extensive changes in linkage distribution compared to the wild-type polysaccharide (**EPS180**). Besides the native (α1→3) and (α1→6) linkages, as present in **EPS180**, a significant amount of (α1→4) linkages is introduced by this mutant enzyme. Here, we report a detailed structural analysis of **mEPS-PNNS**, identifying the structural elements and their quantities, and finally postulating a composite model, that includes all identified structural features.

Experimental Section

Mutant Construction, Enzyme Expression, Purification, and Glucan Synthesis. The triple mutant V1027P:S1137N:A1139S was generated using The QuickChange site-directed mutagenesis kit (Stratagene, LaJolla, CA) and appropriate primer pairs to introduce mutations in p15GTF180-ΔN.[13] After successful mutagenesis (confirmed by nucleotide sequencing), GTF180-ΔN (V1027P:S1137N:A1139S) was overexpressed in *E. coli* BL21star (DE3) and the bioengineered polysaccharide **mEPS-PNNS** was produced by incubation of the His-tag purified enzyme with 146 mM sucrose, containing 1% Tween 80 and 0.02% sodium azide for 7 days.[14] The **mEPS-PNNS** produced was isolated by precipitation with ethanol, as described previously.[15]

Methylation Analysis. Polysaccharide samples were permethylated using CH_3I and solid NaOH in DMSO, as described earlier.[16] After hydrolysis with 2 M TFA (2 h, 120 °C), partially methylated monosaccharide mixtures were reduced with $NaBD_4$ (2 h, room temperature). Conventional workup involving neutralization with HOAc and removal of boric acid by coevaporation with MeOH, followed by acetylation with acetic anhydride−pyridine (1:1 v/v, 3 h, 120 °C), yielded mixtures of partially methylated alditol acetates, which were analyzed by GLC-EI-MS.[17,18]

Partial Acid Hydrolysis. A sample of **mEPS-PNNS** (800 mg) was treated with 0.5 M TFA (2 mL) for 30 min at 90 °C. After centrifugation (1500 *g*, 5 min), the supernatant was collected, and the pellet was treated again with 0.5 M TFA under the same conditions. This procedure was repeated 10 times. Each supernatant was investigated by 1D ^{1}H NMR spectroscopy. Subsequently, the supernatant samples were pooled, profiled on CarboPac PA-100 and separated on Bio-Gel P-2 (400 × 15 mm, BioRad), eluted with 25 mM NH_4HCO_3; 1.2 mL fractions were collected at a flow rate of 11.5 mL/h. Fractions were tested for the

* To whom correspondence should be addressed. E-mail: j.p.kamerling@uu.nl.
[†] Utrecht University.
[‡] University of Groningen.
[§] Centre for Carbohydrate Bioprocessing.

10.1021/bm800410w CCC: $40.75
Published on Web 07/11/2008

presence of carbohydrates by a TLC spot-test with orcinol-H_2SO_4 staining. Carbohydrate-containing fractions were analyzed by MALDI-TOF-MS.

Smith Degradation. A sample of **mEPS-PNNS** (10 mg) was incubated with 2 mL of 50 mM sodium periodate in 0.1 M NaOAc (pH 4.3) for 96 h at 4 °C in the dark. Then the excess of periodate was destroyed by addition of 0.2 mL of ethylene glycol. The oxidized polysaccharide solution was dialysed against tap water (24 h, room temperature), treated with excess $NaBH_4$ (18 h, room temperature), and subsequently neutralized with 4 M HOAc.[19] After coevaporation of boric acid with MeOH, the residue was hydrolyzed with 90% HCOOH (30 min, 90 °C). Finally, the solution was concentrated under a stream of N_2, and the products were analyzed by GLC-EI-MS and HPAEC-PAD.

High-pH Anion-Exchange Chromatography. HPAEC was performed on a Dionex DX500 workstation, equipped with an ED40 pulsed amperometric detection (PAD) system. A triple-pulse amperometric waveform (E_1 0.1 V, E_2 0.7 V, E_3 −0.1 V) was used for detection with the gold electrode.[20] Analytical separations were performed on a CarboPac PA-100 column (250 × 4 mm, Dionex), using a linear gradient of 0−300 mM NaOAc in 100 mM NaOH (1 mL/min). Samples were fractionated on a CarboPac PA-100 column (250 × 9 mm, Dionex), using a linear gradient of 0−300 mM NaOAc in 100 mM NaOH (4 mL/min) or isocratic conditions of 100 mM NaOAc in 100 mM NaOH (4 mL/min). Collected fractions were immediately neutralized with 4 M HOAc, desalted on CarboGraph SPE columns (150 mg graphitised carbon, Alltech) using acetonitrile−H_2O (1:3 v/v) as eluent, and lyophilised.

Mass Spectrometry. GLC-EI-MS was performed on a Fisons Instruments GC 8060/ MD 800 system (Interscience BV; Breda, The Netherlands) equipped with an AT-1 column (30 m × 0.25 mm, Alltech), using a temperature gradient of 140−240 at 4 °C/min.[17]

Matrix-assisted laser desorption ionization time-of-flight mass spectrometry (MALDI-TOF-MS) was carried out on a Voyager-DE Pro (Applied Biosystems; Nieuwerkerk aan de IJssel, The Netherlands) instrument in the reflector mode at an accelerating voltage of 24 kV, using an extraction delay of 90 ns, in a resolution of 5000−9000 FWMH. Samples (1 μL) were mixed in a 1:1 ratio (v/v) with a mixture of 7.5 mg/mL 2,5-dihydroxybenzoic acid in acetonitrile−H_2O (1:1 v/v), and spectra were recorded in the positive-ion mode.

NMR Spectroscopy. 1D/2D ^{1}H NMR spectra were recorded on a Bruker DRX500 spectrometer (Bijvoet Center, Department of NMR spectroscopy, Utrecht University) at a probe temperature of 300 K. Samples were exchanged once with 99.9 atom % D_2O, lyophilised, and dissolved in 650 μL D_2O. ^{1}H chemical shifts (δ) are expressed in ppm by reference to internal acetone (δ 2.225). 1D ^{1}H NMR spectra were recorded with a spectral width of 5000 Hz in 16 k complex data sets and zero-filled to 32 k. A WEFT pulse sequence was applied to suppress the HOD signal.[21] When necessary, a fifth order polynomial baseline correction was applied. 2D TOCSY spectra were recorded using MLEV17 mixing sequences with spin-lock times of 10, 30, 60, 120, and 150 ms. The spin-lock field strength corresponded with a 90° pulse width of about 28 μs at 13 dB. The spectral width in 2D TOCSY experiments was 4006 Hz at 500 MHz in each dimension. The 400−1024 spectra of 2 k data points with 8−32 scans per t_1 increment were recorded. 2D NMR spectroscopic data were analyzed by applying a sinus multiplication window and zero filling to spectra of 4 k by 1 k dimensions. A Fourier transform was applied and, where necessary, a 5 to 15th order polynomial baseline function was applied. All NMR data were processed using in-house developed software (J.A. van Kuik, Bijvoet Center, Department of Bio-Organic Chemistry, Utrecht University).

Results

Composition of mEPS-PNNS. Methylation analysis of **mEPS-PNNS** showed the presence of terminal, 3-, 4-, and 6-substituted, and 3,6-disubstituted glucopyranose in a molar percentage of 18, 10, 12, 42, and 18% (Table 1). 1D ^{1}H NMR spectroscopy of intact **mEPS-PNNS** (Figure 1A) indicated an α-anomeric configuration for all glucose residues. Integration of the anomeric signals revealed 60% (α1→6)-linked D-Glc*p* ($\delta_{H\text{-}1}$ ~4.96), 28% (α1→3)-linked D-Glc*p* ($\delta_{H\text{-}1}$ ~5.33), and 12% (α1→4)-linked D-Glc*p* ($\delta_{H\text{-}1}$ ~5.39) residues, which is in agreement with the overall substitution pattern found by methylation analysis. It should be noted that the low solubility of **mEPS-PNNS** influenced the quality of the 1D ^{1}H NMR spectrum, whereas the broader peaks, compared to the 1D ^{1}H NMR spectrum of wild-type **EPS180**[10] may be the result of a more structural diversity.

Table 1. Methylation Analysis Data of **mEPS-PNNS** Compared with Wild-Type **EPS180**[10] α-D-Glucan[a]

	mEPS-PNNS	EPS180
Glc*p*-(1→	18 ± 1.3[b]	12 ± 0.8
→3)-Glc*p*-(1→	10 ± 1.5	24 ± 0.6
→4)-Glc*p*-(1→	12 ± 1.3	
→6)-Glc*p*-(1→	42 ± 0.8	52 ± 1.3
→3,6)-Glc*p*-(1→	18 ± 1.0	12 ± 1.0

[a] Substitution pattern data are shown in molar percentages based on GLC intensities. [b] Standard deviations have been calculated from multiple methylation analyses of **mEPS-PNNS** and **EPS180**[10] batches. Multiple batches of these EPSs were produced by using mutant and wild-type enzymes, stemming from two separate gene expressions per enzyme.

Partial Acid Hydrolysis. A sample of **mEPS-PNNS** (800 mg) was incubated 10 times with 0.5 M TFA (30 min, 90 °C), with intermediate centrifugation and collection of supernatant. Analysis of the 10 supernatant samples by 1D ^{1}H NMR spectroscopy showed that the proton patterns all resembled that of intact **mEPS-PNNS** (Figure 1A), suggesting that all the structural elements present in **mEPS-PNNS** are also present in the hydrolysates. In each case, the linkage distribution, as determined from the 1D ^{1}H NMR spectra of the 10 batches, amounts to 59% (α1→6) linkages, 28% (α1→3) linkages, and 13% (α1→4) linkages. This indicates that, in contrast with wild-type **EPS180**,[10] all three linkage types are equally susceptible to acid hydrolysis under the conditions selected. For further investigations, the 10 batches were pooled.

HPAEC profiling of the pool on CarboPac PA-100 using a linear gradient showed free glucose (fraction **1**) as the major component (Figure 2A). To obtain suitable fractions for further analysis, a prefractionation was performed on Bio-Gel P-2, yielding 16 overlapping fractions with a broad distribution of fragment sizes (data not shown). On the guidance of MALDI-TOF-MS analysis, the fractions were combined in four subpools as follows: fractions containing fragments with DP ≤ 3 were combined in subpool **I**, fractions containing mostly fragments with DP4−DP7 in subpool **II**, fractions containing mostly fragments with DP8−DP11 in subpool **III**, and fractions containing fragments with DP > 11 in subpool **IV**. Using a linear gradient subpools **I** and **II** were further separated on CarboPac PA-100, yielding fractions **1** to **6** and **7** to **11**, respectively (Figure 2B). Subpools **III** and **IV**, containing fragments too large for a complete ^{1}H NMR analysis were not separated.

Fraction 2. The retention time of fraction **2** on CarboPac PA-100, as well as the 1D ^{1}H NMR spectrum (data not shown) were in agreement with the presence of isomaltose, that is, α-D-Glc*p*-(1→6)-D-Glc*p* (Scheme 1).[22]

Fraction 3. The MALDI-TOF mass spectrum of fraction **3** revealed an $[M + Na]^+$ pseudomolecular ion at *m/z* 527, corresponding with Hex_3. The 1D ^{1}H NMR spectrum (data not shown) matched that of isomaltotriose, that is, α-D-Glc*p*-(1→6)-α-D-Glc*p*-(1→6)-D-Glc*p* (Scheme 1).[22]

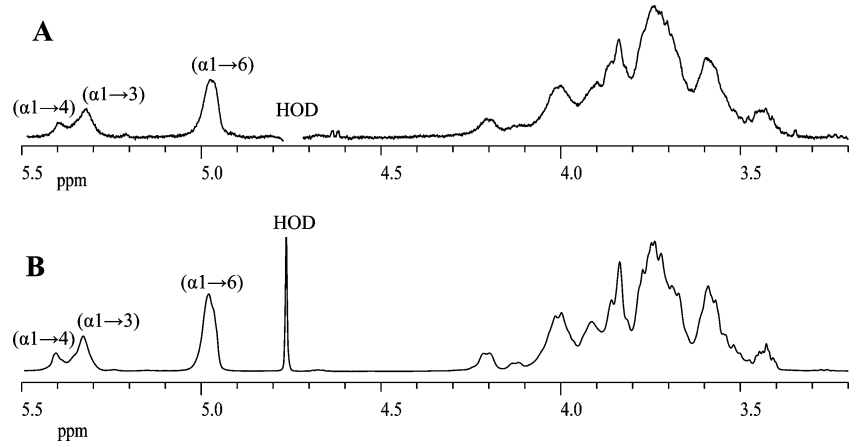

Figure 1. 1D ^{1}H NMR (500 MHz) spectra of (A) **mEPS-PNNS** and (B) **mEPS-PNNS** subpool **IV**, recorded at 300 K in D_2O.

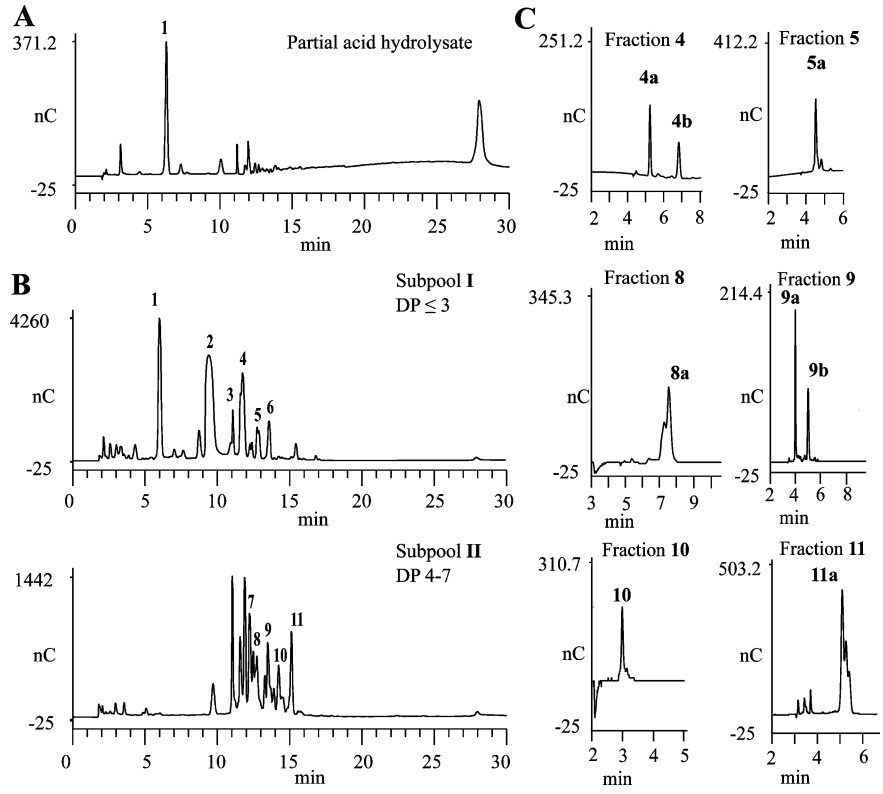

Figure 2. (A) HPAEC profile of **mEPS-PNNS** partial acid hydrolysate on CarboPac PA-100, using a linear gradient; (B) HPAEC profiles of Bio-Gel P-2 subpools **I** and **II** on CarboPac PA-100, using a linear gradient; and (C) HPAEC profiles of HPAEC fractions **4**, **5**, and **8**−**11** on CarboPac PA-100, using isocratic conditions. For experimental details, see Experimental Section.

Fraction 4. MALDI-TOF-MS analysis of fraction **4** showed an $[M + Na]^+$ pseudomolecular ion at *m*/*z* 527, corresponding with Hex_3. However, the separation profile on CarboPac PA-100 (Figure 2B) showed two overlapping peaks. Therefore, fraction **4** was further separated on CarboPac PA-100 under isocratic conditions (Figure 2C), and fractions **4a** and **4b** were isolated. The 1D ^{1}H NMR spectrum of compound **4a** (data not shown) corresponded with that of maltose, that is, α-D-Glc*p*-(1→4)-D-Glc*p*.[22] The 1D ^{1}H NMR spectrum of compound **4b** (data not shown), corresponding with Hex_3 (MALDI-TOF-MS), indicated the presence of panose, that is, α-D-Glc*p*-(1→6)-α-D-Glc*p*-(1→4)-D-Glc*p* (Scheme 1).[22]

Fraction 5. MALDI-TOF-MS analysis of fraction **5** revealed $[M + Na]^+$ pseudomolecular ions at *m*/*z* 527 and 689, corresponding with Hex_3 and Hex_4, respectively. Fraction **5** was further separated on CarboPac PA-100 under isocratic conditions (Figure 2C), rendering one major fraction **5a** (Hex_3, MALDI-TOF-MS).

The 1D ^{1}H NMR spectrum of fraction **5a** (Figure 3A) showed five anomeric signals at δ 5.366 (**B** H-1, $^3J_{1,2}$ 3.4 Hz), 5.246 (**Rα** H-1, $^3J_{1,2}$ 3.4 Hz), 4.962 ($\mathbf{A}_{\beta}$ H-1, $^3J_{1,2}$ 3.4 Hz), 4.955 ($\mathbf{A}_{\alpha}$ H-1, $^3J_{1,2}$ 3.4 Hz), and 4.681 (**Rβ** H-1, $^3J_{1,2}$ 7.8 Hz). The set of **Rα** and **Rβ** H-1 values corresponds with the occurrence of a -(1→6)-D-Glc*p* unit in a -(1→3)-α-D-Glc*p*-(1→6)-D-Glc*p* sequence (library data: -(1→3)-α-D-Glc*p*-(1→6)-D-Glc*p*, δ 5.246−5.249 and 4.676−4.680; -(1→4/6)-α-D-Glc*p*-(1→6)-D-Glc*p*, δ 5.240−5.241 and 4.667−4.672).[10,11,22] The presence of **Rα** H-6b at δ 3.966 is in agreement with a 6-substituted residue **R**. The splitting of **A** H-1 is due to the influence of the α/β configuration of the reducing residue **R**. The **B** H-1 signal at δ

Scheme 1. Structures of Oligosaccharide Fragments Obtained by Partial Acid Hydrolysis of **mEPS-PNNS**

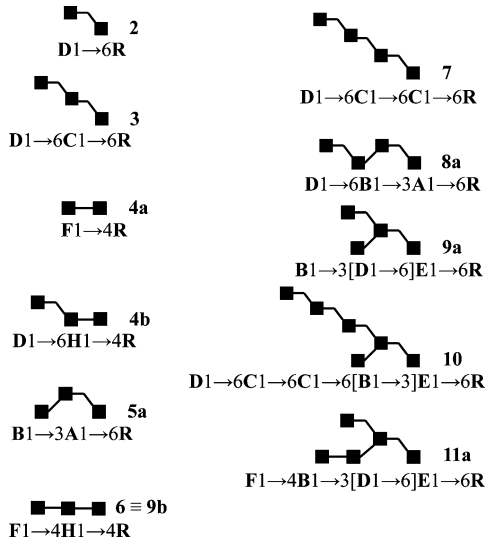

5.366 corresponds with that of an (-)α-D-Glc*p*-(1→3)- unit.[22] The **B** H-4 signal at δ 3.451 was established as a structural-reporter-group signal of a terminal α-D-Glc*p*-(1→*x*)- unit,[22] and has a surface area corresponding to one proton, indicating a linear structure. These data lead to a **B**1→3**A**1→6**R** sequence for compound **5a**, that is, α-D-Glc*p*-(1→3)-α-D-Glc*p*-(1→6)-D-Glc*p* (Scheme 1). (For Glc residues at semidefined places in the structure (-)α-D-Glc*p*-(1→*x*)- or -(1→*x*)-α-D-Glc*p*(-) is used. When the structural context of the residue is precisely known, this is indicated as follows: -(1→*x*)-α-D-Glc*p*-(1→*y*)-, describing an *x*-substituted residue with a (1→*y*) linkage. In the case of a nonreducing terminal residue α-D-Glc*p*-(1→*x*)- is used, a reducing terminal residue is indicated with -(1→*x*)-D-Glc*p*.)

Fraction 6. MALDI-TOF-MS and ^{1}H NMR analysis (data not shown) of fraction **6** demonstrated the presence of maltotriose, that is, α-D-Glc*p*-(1→4)-α-D-Glc*p*-(1→4)-D-Glc*p* (Scheme 1).[22]

Fraction 7. The MALDI-TOF mass spectrum of fraction **7** revealed an $[M + Na]^+$ pseudomolecular ion at *m/z* 689, corresponding with Hex_4. The 1D ^{1}H NMR spectrum (data not shown) matched that of isomaltotetraose, that is, α-D-Glc*p*-(1→6)-α-D-Glc*p*-(1→6)-α-D-Glc*p*-(1→6)-D-Glc*p*.[10]

Fraction 8. MALDI-TOF-MS analysis of fraction **8** showed $[M + Na]^+$ pseudomolecular ions at *m/z* 527 and 689, corresponding with Hex_3 and Hex_4, respectively. Fraction **8** was further separated on CarboPac PA-100, using 100 mM NaOAc in 100 mM NaOH (Figure 2C), yielding the major fraction **8a** (Hex_4, MALDI-TOF-MS).

The 1D ^{1}H NMR spectrum (data not shown) of fraction **8a** showed five anomeric signals at δ 5.345/5.336 (**B** H-1, $^3J_{1,2}$ 3.6 Hz), 5.249 (**Rα** H-1, $^3J_{1,2}$ 3.6 Hz), 4.965 (**D** H-1, $^3J_{1,2}$ 3.6 Hz), 4.958 (**A** H-1, $^3J_{1,2}$ 3.6 Hz), and 4.680 (**Rβ** H-1, $^3J_{1,2}$ 7.8 Hz). Assignments of nonanomeric proton chemical shifts (Table 2) were obtained from 2D ^{1}H−^{1}H TOCSY measurements (data not shown). In fact, the various NMR data match exactly with those obtained from **EPS180** compound **3b**, identified previously:[10] **D**1→6**B**1→3**A**1→6**R**, that is, α-D-Glc*p*-(1→6)-α-D-Glc*p*-(1→3)-α-D-Glc*p*-(1→6)-D-Glc*p* (Scheme 1).

Fraction 9. Analysis of fraction **9** by MALDI-TOF-MS revealed $[M + Na]^+$ pseudomolecular ions at *m/z* 527 and 689, corresponding with Hex_3 and Hex_4, respectively. Fraction **9** was further separated on CarboPac PA-100, under isocratic conditions (Figure 2C), yielding a major fraction **9a** (Hex_4; MALDI-TOF-MS) and a minor fraction **9b** (Hex_3; MALDI-TOF-MS).

The 1D ^{1}H NMR spectrum of Hex_4 **9a** (Figure 4) showed six anomeric signals at δ 5.353 ($\mathbf{B}_\alpha$ H-1, $^3J_{1,2}$ 3.8 Hz), 5.343 ($\mathbf{B}_\beta$ H-1, $^3J_{1,2}$ 3.8 Hz), 5.249 (**Rα** H-1, $^3J_{1,2}$ 3.8 Hz), 4.975 (**E** H-1, $^3J_{1,2}$ 3.8 Hz), 4.965 (**D** H-1, $^3J_{1,2}$ 3.8 Hz), and 4.683 (**Rβ** H-1, $^3J_{1,2}$ 7.6 Hz). 2D ^{1}H−^{1}H TOCSY measurements (Figure 4/60 ms) delivered most of the δ values of the nonanomeric protons (Table 2). The chemical shift positions of **Rα** and **Rβ** H-1 at δ 5.249 and 4.683, respectively, correspond with the occurrence of a -(1→6)-D-Glc*p* unit in a -(1→3)-α-D-Glc*p*-(1→6)-D-Glc*p* sequence.[10,11,22] This is further corroborated by the **Rβ** H-2 signal at δ 3.258, indicating that residue **R** is not 3- or 4-substituted.[22] The split **B** H-1 signal at δ 5.353/5.343 fits best with the occurrence of an (-)α-D-Glc*p*-(1→3)- unit.[10,22] The set of **B** H-4 and H-5 at δ 3.45 and 4.00, respectively, identified residue **B** as a terminal α-D-Glc*p*-(1→3)- unit (see nigerose residue **B** and nigerotriose residue **C** in ref 22). Residue **D** H-1 at δ 4.965 is indicative of an (-)α-D-Glc*p*-(1→6)- unit, and together with **D** H-4 at δ 3.43, a terminal α-D-Glc*p*-(1→6)- unit is demonstrated.[22] The occurrence of two terminal units indicates a branched structure for **9a**. Finally, the **E** H-1 signal at δ 4.975 revealed the occurrence of an (-)α-D-Glc*p*-(1→6)- unit. Because residue **R** is not 3-substituted, the remaining internal residue **E** has to be a 3,6-disubstituted unit, yielding the sequence of **9a**: **B**1→3[**D**1→6]**E**1→6**R**, that is, α-D-Glc*p*-(1→3)-[α-D-Glc*p*-(1→6)-]α-D-Glc*p*-(1→6)-D-Glc*p* (Scheme 1).

The 1D ^{1}H NMR spectrum of trisaccharide **9b** matched that of maltotriose, that is, α-D-Glc*p*-(1→4)-α-D-Glc*p*-(1→4)-D-Glc*p* (Scheme 1).[22]

Fraction 10. MALDI-TOF-MS analysis of fraction **10** revealed an $[M + Na]^+$ pseudomolecular ion at *m/z* 1013, corresponding with Hex_6. The 1D ^{1}H NMR spectrum (Figure 5) showed anomeric signals at δ 5.36 ($\mathbf{B}_\alpha$ H-1), 5.34 ($\mathbf{B}_\beta$ H-1), 5.246 (**Rα** H-1), 4.96−4.98 ($\mathbf{C}^{\mathbf{I,II}}$ H-1, **D** H-1, **E** H-1), and 4.679 (**Rβ** H-1, $^3J_{1,2}$ 7.8 Hz). The chemical shift values of the nonanomeric protons (Table 2) were obtained from 2D ^{1}H−^{1}H TOCSY measurements (Figure 5/60 ms). The **Rα** and **Rβ** H-1 δ values at 5.246 and 4.679 ppm, respectively, correspond with the presence of a -(1→6)-D-Glc*p* unit in a -(1→3)-α-D-Glc*p*-(1→6)-D-Glc*p* sequence.[10,11,22] The **Rβ** H-2 signal at δ 3.259, indicating that residue **R** is not 3- or 4-substituted (library data: **Rβ** in nigerose $\delta_{H\text{-}2}$ 3.332 and **Rβ** in maltose $\delta_{H\text{-}2}$ 3.272), supports this conclusion.[22] The set of **B** H-1, H-2, H-3, and H-4 values corresponds with that of **B** in **9a**, revealing the occurrence of a terminal α-D-Glc*p*-(1→3)- unit. The presence of the set of **D** H-1 and H-4 at δ ∼4.97 and 3.42, respectively, indicates the presence of a terminal α-D-Glc*p*-(1→6)- unit. The presence of two terminal units implicates a branched structure for compound **10** (Hex_6). Because the H-1 signal at δ 4.96−4.98, typical for (-)α-D-Glc*p*-(1→6)- residues, corresponds to four protons and residue **R** is not 3-substituted, the structure has to contain an internal 3,6-disubstituted residue **E** (compare with **9a**). Then, the remaining two residues can only be internal -α-D-Glc*p*-(1→6)- units, denoted residue $\mathbf{C}^{\mathbf{I}}$ and $\mathbf{C}^{\mathbf{II}}$. Because the **B** H-1 signal is split, due to the influence of the reducing residue α/β configuration, the most probable sequence for compound **10** is **D**1→6$\mathbf{C}^{\mathbf{II}}$1→6$\mathbf{C}^{\mathbf{I}}$1→6[**B**1→3]**E**1→6**R**, that is, α-D-Glc*p*-(1→6)-α-D-Glc*p*-(1→6)-α-D-Glc*p*-(1→6)-[α-D-Glc*p*-(1→3)-]α-D-Glc*p*-(1→6)-D-Glc*p* (Scheme 1).

Fraction 11. MALDI-TOF-MS analysis of fraction **11** showed $[M + Na]^+$ pseudomolecular ions at *m/z* 851 and 1013, corresponding with Hex_5 and Hex_6, respectively. Fraction **11** was further separated on CarboPac PA-100, under isocratic conditions (Figure 2C), yielding one major fraction **11a** (Hex_5, MALDI-TOF-MS).

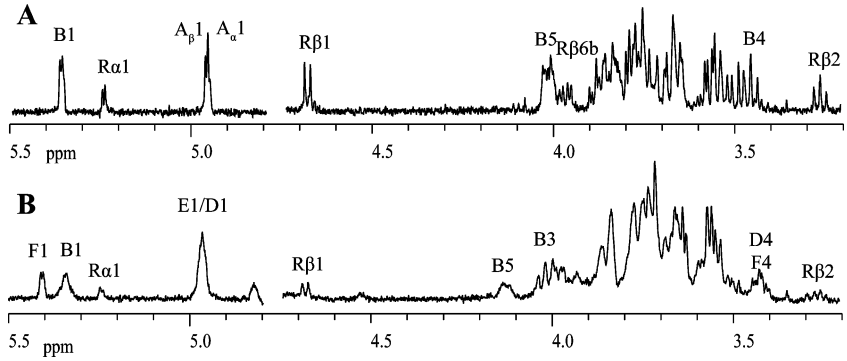

Figure 3. 1D ^{1}H NMR spectra (500 MHz) of (A) fraction **5a** and (B) fraction **11a**, recorded at 300 K in D_2O. Structural-reporter-group signals that could be distinguished are indicated in the spectra. Labels correspond with those used in Table 2 and Scheme 1.

Table 2. ^{1}H Chemical Shifts of D-Glucopyranose Residues of Oligosaccharide Fragments Obtained by Partial Acid Hydrolysis of **mEPS-PNNS**[a]

residue	8a	9a	10
Rα-1	5.249	5.249	5.246
Rα-2	3.54	3.54	n.d.
Rα-3	3.71	3.71	n.d.
Rα-4	3.51	3.52	n.d.
Rα-5	4.00	4.01	n.d.
R*β*-1	4.680	4.683	4.679
R*β*-2	3.258	3.258	3.259
R*β*-3	3.49	3.49	n.d.
R*β*-4	3.52	3.51	n.d.
R*β*-5	3.65	3.65	n.d.
A-1	4.958		
A-2	3.65		
A-3	3.84		
A-4	3.67		
B-1	5.345/336	5.353/343	5.36/34
B-2	3.58	3.57	3.58
B-3	3.75	3.75	3.75
B-4	3.51	3.45	3.45
B-5	4.20	4.00	n.d.
C-1			∼4.97
C-2			3.57
C-3			3.74
D-1	4.965	4.965	∼4.97
D-2	3.55	3.55	3.57
D-3	3.75	3.75	3.74
D-4	3.42	3.43	3.42
D-5	n.d.	3.76	n.d.
E-1		4.975	∼4.97
E-2		3.65	3.65
E-3		3.86	3.88
E-4		3.76	n.d.
E-5		3.92	n.d.

[a] Residue labels correspond to those used in Scheme 1.

The 1D ^{1}H NMR spectrum of fraction **11a** (Figure 3B) showed anomeric signals at δ 5.410 (**F** H-1, $^3J_{1,2}$ 3.6 Hz; (α1→4) linkage), 5.35−5.36 (**B** H-1; (α1→3) linkage), 5.247 (**R**α H-1), 4.97−4.99 (**D** H-1, **E** H-1; (α1→6) linkages), and 4.681 (**R***β* H-1, $^3J_{1,2}$ 7.6 Hz). The H-1α and H-1*β* chemical shifts of the reducing residue **R** at δ 5.247 and 4.681, respectively, correspond with the occurrence of a -(1→6)-D-Glc*p* unit in a -(1→3)-α-D-Glc*p*-(1→6)-D-Glc*p* sequence.[10,11,22] The occurrence of the signal at $\delta_{H\text{-}4}$ 3.42 (dd, 2 H), being indicative for an α-D-Glc*p*-(1→*x*)- unit,[22] reflects a branched structure. As an H-5 signal at δ 4.20 is missing, the occurrence of a -(1→6)-α-D-Glc*p*-(1→3)- unit can be excluded.[10] However, a signal at δ 4.12 is observed with a characteristic peak-shape of an H-5 signal, significantly downfield from H-5 of an α-D-Glc*p*-(1→3)- unit (see also residue **B** in **9a**),[22] which can be explained by the effect of a 4-substitution on an α-D-Glc*p*-(1→3)- unit ($\Delta\delta_{H\text{-}5}$ +0.10−0.14 ppm, ref 22), leading to the presence of a -(1→4)-α-D-Glc*p*-**B**-(1→3)- unit. This observation adds a new structural-reporter-group signal to the concept.[10,11,22] These data lead to a structural element **F**1→4**B**1→3**E**1→6**R**. The final residue **D** has to be positioned to cause a branched structure, which can only occur at residue **E**, resulting in an **F**1→4**B**1→3[**D**1→6]**E**1→6**R** sequence for compound **11a**, that is, α-D-Glc*p*-(1→4)-α-D-Glc*p*-(1→3)-[α-D-Glc*p*-(1→6)-]α-D-Glc*p*-(1→6)-D-Glc*p* (Scheme 1).

Smith Degradation. To investigate the degree of polymerization of (α1→3) glycosidic bonds, **mEPS-PNNS** was subjected to a Smith degradation, comprising a periodate oxidation, followed by reduction with $NaBH_4$, and mild acid hydrolysis with formic acid. The formed products were analyzed by GLC-EI-MS and HPAEC-PAD. In view of the linkage analysis of **mEPS-PNNS** (see above), α-D-Glc*p*-(1→1)-Gro and [α-D-Glc*p*-(1→3)-]$_n$α-D-Glc*p*-(1→1)-Gro, but also, due to excessive hydrolysis, Gro, D-Glc, and [α-D-Glc*p*-(1→3)-]$_n$D-Glc can be expected.

GLC-EI-MS analysis (data not shown) of the trimethylsilylated residue showed three major products: Gro, D-Glc*p*, and α-D-Glc*p*-(1→1)-Gro. Typical fragments for α-D-Glc*p*-(1→1)-Gro are *m*/*z* 451 (aA_1), 361 (aA_2), 271 (aA_3), 217, and 204 for the Glc moiety, and *m*/*z* 219 (bA_1) and 337 (abJ_1) for the Gro moiety.[17,23–25]

HPAEC analysis on CarboPac PA-100 (data not shown) of the residue revealed two major peaks that could be related to Gro (R_t 2.2 min) and α-D-Glc*p*-(1→1)-Gro (R_t 6.2 min), which was identified by its elution position, being slightly later than D-Glc*p* (R_t 5.6 min). Because α-D-Glc*p*-(1→3)-D-Glc*p* under the same conditions has an R_t value >10 min, the presence of [α-D-Glc*p*-(1→3)-]$_n$α-D-Glc*p*-(1→1)-Gro with $n = 1$ or higher could be excluded.

The absence of structures larger than glucosyl-glycerol indicates that the **mEPS-PNNS** structure does not contain two or more consecutive (α1→3) linkages, similar to the wild-type **EPS180**.[10]

2D NMR Analysis of mEPS-PNNS Using Subpool IV. Intact **mEPS-PNNS** does not dissolve in suitable amounts to allow 2D NMR analysis. As the ^{1}H NMR spectrum of subpool **IV**, isolated from a partial hydrolysate of **mEPS-PNNS** and containing fragments of DP >11, is similar to that of intact **mEPS-PNNS** (Figure 1A,B), this subpool was subjected to 2D NMR analysis. Especially, the larger oligosaccharides in subpool **IV** are suitable to represent all the structural elements that are present in the full length polysaccharide and do not have interfering signals from reducing residues. 2D ^{1}H−^{1}H TOCSY experiments with increasing mixing times (10, 30, 60, 120, and 150 ms) were interpreted (Figure 6; 60 and 120 ms) to unravel the structural elements present in **mEPS-PNNS**. In several cases, use is made of the ^{1}H NMR data

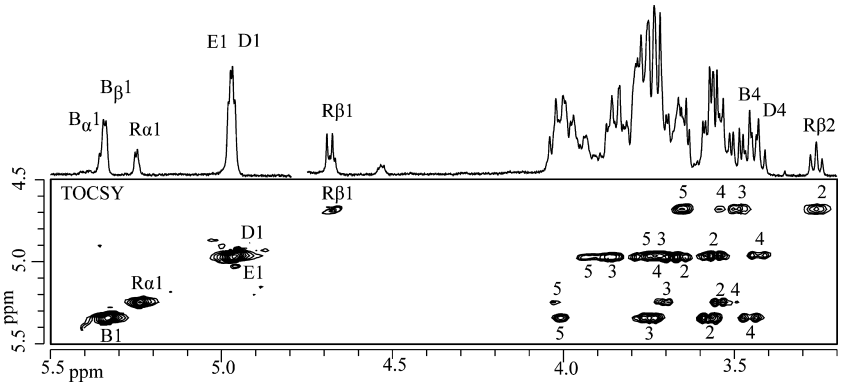

Figure 4. 1D ^{1}H NMR (500 MHz) spectrum and the relevant part of the 2D ^{1}H−^{1}H TOCSY spectrum (60 ms) of fraction **9a**, recorded at 300 K in D_2O. Anomeric protons in the TOCSY spectrum (Rα1, etc.) have been indicated on the diagonal; numbers in the horizontal tracks belong to the cross-peaks of the scalar-coupling network of the residues indicated.

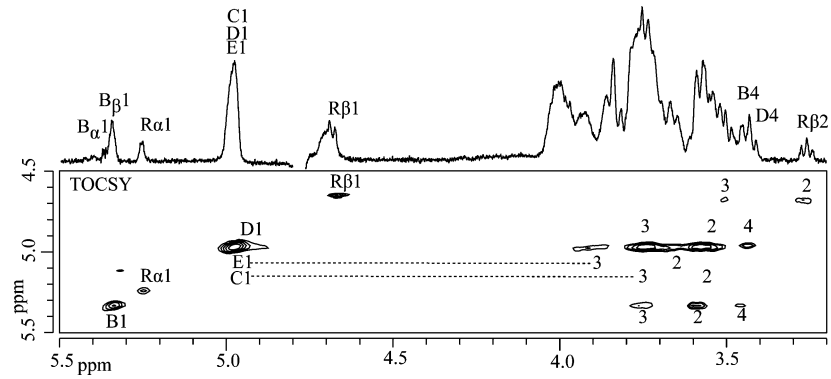

Figure 5. 1D ^{1}H NMR (500 MHz) spectrum and the relevant part of the 2D ^{1}H−^{1}H TOCSY spectrum (60 ms) of fraction **10**, recorded at 300 K in D_2O. For an explanation of the coding system, see Figure 4.

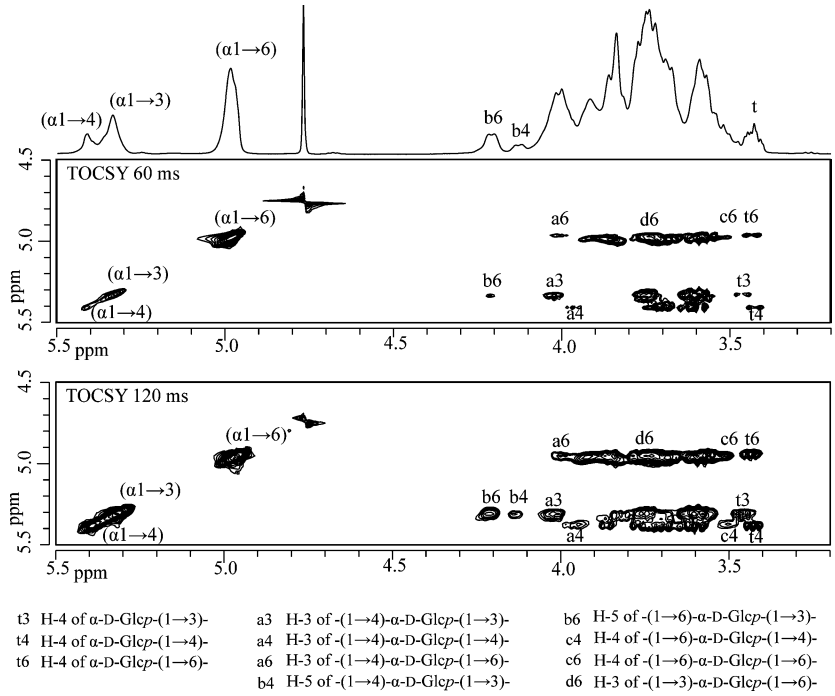

t3 H-4 of α-D-Glc*p*-(1→3)-
t4 H-4 of α-D-Glc*p*-(1→4)-
t6 H-4 of α-D-Glc*p*-(1→6)-
a3 H-3 of -(1→4)-α-D-Glc*p*-(1→3)-
a4 H-3 of -(1→4)-α-D-Glc*p*-(1→4)-
a6 H-3 of -(1→4)-α-D-Glc*p*-(1→6)-
b4 H-5 of -(1→4)-α-D-Glc*p*-(1→3)-
b6 H-5 of -(1→6)-α-D-Glc*p*-(1→3)-
c4 H-4 of -(1→6)-α-D-Glc*p*-(1→4)-
c6 H-4 of -(1→6)-α-D-Glc*p*-(1→6)-
d6 H-3 of -(1→3)-α-D-Glc*p*-(1→6)-

Figure 6. 1D ^{1}H NMR (500 MHz) spectrum and the relevant parts of the 2D ^{1}H−^{1}H TOCSY spectra (upper 60 ms, lower 120 ms) of **mEPS-PNNS** subpool **IV**, recorded at 300 K in D_2O. Anomeric signals and structural-reporter-group signals have been indicated with labels; the legend to the labels used is included.

collected from the oligosaccharides obtained by partial acid hydrolysis of **mEPS-PNNS**, as well as from data reported in refs 10, 11, and 22.

So far (refs 11 and 22, this study), depending on the microenvironment of the unit, the δ value of the H-1 signal of a (-)α-D-Glc*p*-(1→4)- unit varies between 5.41 and 5.33 ppm. In a similar way, the δ value of the H-1 signal of a (-)α-D-Glc*p*-(1→3)- unit was found to lie between 5.39 and 5.32 ppm (refs 10 and 22, this study). This means that the anomeric signal of (α1→4)-linked residues could overlap with the anomeric

Table 3. Percentages of Building Blocks Present in **mEPS-PNNS** and Wild-Type **EPS180**[10] α-D-Glucans

building block	residue	mEPS-PNNS	EPS180
-(1→3)-α-D-Glc*p*-(1→6)-	**A**	10	19
α-D-Glc*p*-(1→3)-	^{t}**B**	4	0
-(1→4)-α-D-Glc*p*-(1→3)-	^{4}**B**	7	0
-(1→6)-α-D-Glc*p*-(1→3)-	^{6}**B**	17	31
-(1→4)-α-D-Glc*p*-(1→6)-	^{4}**C**	2	0
-(1→6)-α-D-Glc*p*-(1→6)-	^{6}**C**	22	26
α-D-Glc*p*-(1→6)-	**D**	8	12
-(1→3,6)-α-D-Glc*p*-(1→6)-	**E**	18	12
α-D-Glc*p*-(1→4)-	**F**	6	0
-(1→4)-α-D-Glc*p*-(1→4)-	^{4}**H**	3	0
-(1→6)-α-D-Glc*p*-(1→4)-	^{6}**H**	3	0

signal of (α1→3)-linked residues. In the 1D ^{1}H NMR spectrum of subpool **IV** (Figure 1B), the H-1 signal between δ 5.41 and 5.39 has a surface area matching the amount of (α1→4)-linked residues, as derived from the substitution pattern determined by methylation analysis, and can therefore be considered as the (α1→4)-anomeric signal. This means that the peak between δ 5.39 and 5.32 corresponds with (α1→3)-linked residues. The peak at δ 4.96 is a typical structural reporter for (-)α-D-Glc*p*-(1→6)- units (δ-range between 4.99 and 4.95 ppm, refs 10, 11, and 22, this study).

In the 60 ms TOCSY spectrum of subpool **IV** (Figure 6), the H-1 track of (-)α-D-Glc*p*-(1→3)- residues (δ 5.39−5.32) showed a characteristic H-3 signal at δ 4.01, reflecting the occurrence of -(1→4)-α-D-Glc*p*-(1→3)- units (compare with -(1→4)-α-D-Glc*p*-(1→4)-, $\delta_{H\text{-}3}$ 3.96; -(1→4)-α-D-Glc*p*-(1→6)-, $\delta_{H\text{-}3}$ 4.01).[11,22] This is further confirmed by the H-5 resonance at δ 4.12 (see compound **11a**) in the 120 ms TOCSY spectrum (Figure 6). On the same track in the 120 ms TOCSY spectrum, another H-5 resonance at δ 4.20 is observed, corresponding with -(1→6)-α-D-Glc*p*-(1→3)- units.[10] The presence of terminal α-D-Glc*p*-(1→3)- units is indicated by the presence of the signal at δ 3.45 (H-4), an established structural reporter for terminal residues.[22] The absence of $\delta_{H\text{-}3}$ ~3.90 on this track, indicates that -(1→3)-α-D-Glc*p*-(1→3)- units do not occur in **mEPS-PNNS**.[22]

On the H-1 track of the (-)α-D-Glc*p*-(1→4)- residues in the 60 ms TOCSY spectrum (Figure 6) a weak H-3 resonance was detected at δ 3.96, indicating a minor occurrence of -(1→4)-α-D-Glc*p*-(1→4)- units (see residue **B** in maltotriose[22] and residue **H** in **6** and **9b**). A stronger H-3 signal at δ 3.70 indicates a major occurrence of -(1→6)-α-D-Glc*p*-(1→4)- and/or terminal α-D-Glc*p*-(1→4)- units. The structural-reporter-group signal for terminal residues at $\delta_{H\text{-}4}$ 3.42 is also observed on this track, confirming the presence of α-D-Glc*p*-(1→4)- units. The occurrence of minor amounts of -(1→6)-α-D-Glc*p*-(1→4)- is reflected by the weak H-4 resonance at δ 3.50, observed in the 120 ms TOCSY spectrum (Figure 6; see also residue **B** in panose,[22] and residue **D** in **4b**). The absence of $\delta_{H\text{-}3}$ ~3.90 (see residue **B** in nigerotriose)[22] suggests that -(1→3)-α-D-Glc*p*-(1→4)- units do not occur in **mEPS-PNNS**.

On the (-)α-D-Glc*p*-(1→6)- H-1 track in the 30 ms TOCSY spectrum (data not shown) $\delta_{H\text{-}3}$-values were observed at 3.75, 3.85, and 4.00 ppm, respectively. The first value corresponds with the occurrence of α-D-Glc*p*-(1→6)- and/or -(1→6)-α-D-Glc*p*-(1→6)- units,[22] the second indicates the occurrence of -(1→3)-α-D-Glc*p*-(1→6)- and/or -(1→3,6)-α-D-Glc*p*-(1→6)- units,[10] and the third is indicative for the presence of -(1→4)-α-D-Glc*p*-(1→6)- units (compare residue **B** in compounds **3a**, **5a**, **6a**, and **7a** in ref 11). The occurrence of terminal α-D-Glc*p*-(1→6)- is further supported by the presence of an H-4 resonance at δ 3.43 on the (α1→6)-anomeric track. The -(1→6)-α-D-Glc*p*-(1→6)- moiety was shown to occur by the presence of $\delta_{H\text{-}4}$ 3.50 on the same track.[10,22]

Discussion and Conclusions

Building blocks and their quantities were determined by combining data obtained from methylation analysis and Smith degradation analysis of intact **mEPS-PNNS**, from ^{1}H NMR spectroscopy of intact **mEPS-PNNS** and its subpool **IV**, as well as from MS and ^{1}H NMR analysis of oligosaccharides obtained by partial acid hydrolysis of **mEPS-PNNS**.

mEPS-PNNS turned out to contain 28% (α1→3)-linked D-Glc*p* (**B**). From integration of the H-5 signals of -(1→6)-α-

Scheme 2. Composite Model of the **mEPS-PNNS** α-D-Glucan[a]

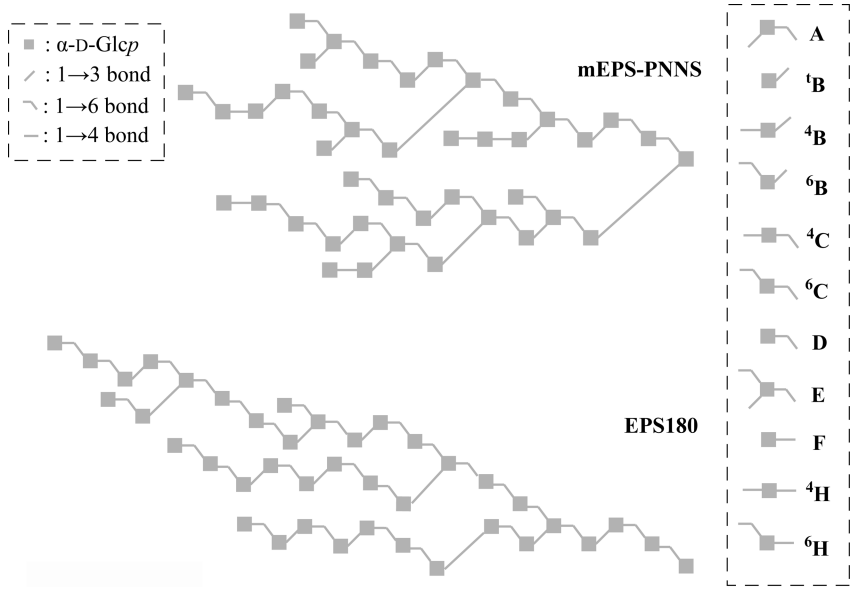

[a] The composite takes into account all facts from the methylation analysis of **mEPS-PNNS**, the Smith degradation study of **mEPS-PNNS**, and the various ^{1}H NMR analyses of **mEPS-PNNS** (subpool IV) and its established fragments. Residue labels correspond with those used in the text, tables, and figures and are represented on the right. For comparison, the composite model of the wild-type **EPS180** α-D-glucan is included.

D-Glc*p*-(1→3)- (^{6}**B**; δ 4.20) and -(1→4)-α-D-Glc*p*-(1→3)- (^{4}**B**; δ 4.12) in the 1D ^{1}H NMR spectrum, the occurrence of these building blocks was quantified at 17 and 7%, respectively (Table 3). This leaves 4% for the remaining α-D-Glc*p*-(1→3)- unit (^{t}**B**; Table 3).

The original structural limitation of single (α1→3) bridges in **EPS180**[10] exists also in **mEPS-PNNS**. Because (-)α-D-Glc*p*-(1→4)- units were not 3-substituted, all 3-substituted Glc*p* residues (10%) are in fact -(1→3)-α-D-Glc*p*-(1→6)- (**A**). Furthermore, methylation analysis indicated 18% 3,6-disubstituted Glc*p*, which means 18% of all residues are -(1→3,6)-α-D-Glc*p*-(1→6)- (**E**; Table 3).

In accordance with 18% branching, 18% terminal residues also do occur. As mentioned above, 4% of these residues were α-D-Glc*p*-(1→3)- units (^{t}**B**). Because the H-4 resonance at δ 3.42−3.43, indicative for terminal residues,[10,11,22] on the (α1→6)-anomeric track was stronger than on the (α1→4)-anomeric track, the occurrence of α-D-Glc*p*-(1→6)- (**D**) and α-D-Glc*p*-(1→4)- (**F**) will be around 8 and 6%, respectively.

With a total of 12% (α1→4)-linked residues (**F**+**H**) and the estimated 6% for α-D-Glc*p*-(1→4)- units (**F**), an amount of 6% is left for -(1→4)-α-D-Glc*p*-(1→4)- (^{4}**H**) and -(1→6)-α-D-Glc*p*-(1→4)- (^{6}**H**). Methylation analysis showed 12% 4-substituted Glc*p*. Taking into account that already 7% -(1→4)-α-D-Glc*p*-(1→3)- units (^{4}**B**) were assigned (see above), 5% is left for both -(1→4)-α-D-Glc*p*-(1→4)- units (^{4}**H**) and -(1→4)-α-D-Glc*p*-(1→6)- units (^{4}**C**). Based on TOCSY cross-peak intensities, the amounts -(1→4)-α-D-Glc*p*-(1→4)- (H-3), -(1→6)-α-D-Glc*p*-(1→4)- (H-4), and -(1→4)-α-D-Glc*p*-(1→6)- (H-3) units will be about 3, 3, and 2%, respectively (Table 3).

With the building blocks that could be determined from the available ^{1}H NMR and methylation analysis data, only one possible building block is left undetermined, that is, -(1→6)-α-D-Glc*p*-(1→6)- units (^{6}**C**), which can then be determined indirectly (22%) from the methylation analysis.

When the building block quantities and the sequences found for the different oligosaccharides are used, a composite model that includes all estasblished structural features can be formulated as depicted in Scheme 2. For comparison, the earlier formulated composite model of wild-type **EPS180**[10] is included in Scheme 2, whereas the percentages of building blocks are given in Table 3.

The composite model shows a more complex structure for **mEPS-PNNS** compared to wild-type **EPS180**. The presence of (α1→4) di- and trisaccharide elements shows that the amino acid mutations in the GTF180 enzyme have significantly changed its structural selectivity. However, the original structural limitation of single (α1→3) bridges still exists. The presence of (α1→6)-linked elements up to five residues in a row (compound **10**) indicates that the isomalto-oligosaccharide basis of the structure also still exists. The maximum length of (α1→6)-linked stretches was not determined in wild-type **EPS180** and also cannot be determined in the case of **mEPS-PNNS**. The different linkage distribution in the **mEPS-PNNS** structure puts a limit on the maximum length of the (α1→6)-linked elements, however, it must be shorter than that in wild-type **EPS180**. The **mEPS-PNNS** polysaccharide is less soluble than the wild-type **EPS180**. The lower solubility is probably the result of a more rigid structure, since (α1→6) linkages are flexible, whereas (α1→3) and (α1→4) are more rigid.[26] Increased rigidity of the structure may also cause the higher resistance to acid hydrolysis that was observed.

Acknowledgment. We thank the Ministry of Economic Affairs (Senter Novem; Bioprimer/project EETK 01129) for financial support.

References and Notes

(1) Costerton, J. W.; Cheng, K.-J.; Geesey, G. G.; Ladd, T. I.; Nickel, J. C.; Dasgupta, M.; Marrie, T. J. *Annu. Rev. Microbiol.* **1987**, *41*, 435–464.
(2) Ceri, H.; McArthur, H. A. I.; Whitfield, C. *Infect. Immun.* **1986**, *51*, 1–5.
(3) Sandford, P. A.; Baird, J. In *The Polysaccharides*; Aspinall, G. O., Ed.; Academic Press: New York, 1983; Vol. 2, pp 411−490.
(4) Sutherland, I. W. *Pure Appl. Chem.* **1997**, *69*, 1911–1917.
(5) Staaf, M.; Yang, Z.; Huttunen, E.; Widmalm, G. *Carbohydr. Res.* **2000**, *236*, 113–119.
(6) Skjåk-Bræk, G.; Smidsrød, O.; Larsen, B. *Int. J. Biol. Macromol.* **1986**, *8*, 330–336.
(7) McCleary, B. V.; Dea, I. C. M.; Windust, J.; Cooke, D. *Carbohydr. Polym.* **1984**, *4*, 253–270.
(8) Breedveld, M.; Bonting, K.; Dijkhuizen, L. *FEMS Microbiol. Lett.* **1998**, *169*, 241–249.
(9) Stingele, F.; Neeser, J.-R.; Mollet, B. *J. Bacteriol.* **1996**, *178*, 1680–1690.
(10) Van Leeuwen, S. S.; Kralj, S.; van Geel-Schutten, G. H.; Gerwig, G. J.; Dijkhuizen, L.; Kamerling, J. P. *Carbohydr. Res.* **2008**, *343*, 1237–1250.
(11) Van Leeuwen, S. S.; Kralj, S.; van Geel-Schutten, G. H.; Gerwig, G. J.; Dijkhuizen, L.; Kamerling, J. P. *Carbohydr. Res.* **2008**, *343*, 1251–1256.
(12) Kralj, S.; van Geel-Schutten, G. H.; Faber, E. J.; van der Maarel, M. J. E. C.; Dijkhuizen, L. *Biochemistry* **2005**, *44*, 9206–9216.
(13) Kralj, S.; van Geel-Schutten, G. H.; Dondorff, M. M. G.; Kirsanovs, S.; van der Maarel, M. J. E. C.; Dijkhuizen, L. *Microbiology* **2004**, *150*, 3681–3690.
(14) Pijning, T.; Vujičić-Žagar, A.; Kralj, S.; Eeuwema, W.; Dijkhuizen, L.; Dijkstra, B. W. *Biocatal. Biotransform.* **2008**, *26*, 12–17.
(15) Van Geel-Schutten, G. H.; Faber, E. J.; Smit, E.; Bonting, K.; Smith, M. R.; Ten Brink, B.; Kamerling, J. P.; Vliegenthart, J. F. G.; Dijkhuizen, L. *Appl. Environ. Microbiol.* **1999**, *276*, 44557–44562.
(16) Ciucanu, I.; Kerek, F. *Carbohydr. Res.* **1984**, *131*, 209–217.
(17) Kamerling, J. P.; Vliegenthart, J. F. G. In *Clinical Biochemistry - Principles, Methods, Applications. Vol. 1, Mass Spectrometry*; Lawson, A. M., Ed.; Walter de Gruyter: Berlin 1989; pp 176−263.
(18) Jansson, P.-E.; Kenne, L.; Liedgren, H.; Lindberg, B.; Lönngren, J. *Chem. Commun. (Stockholm Univ.)* **1976**, *8*, 1–74.
(19) Hay, G. W.; Lewis, B. A.; Smith, F. *Methods Carbohydr. Chem.* **1965**, *5*, 357–360.
(20) Lee, Y. C. *Anal. Biochem.* **1990**, *189*, 151–162.
(21) Hård, K.; van Zadelhoff, G.; Moonen, P.; Kamerling, J. P.; Vliegenthart, J. F. G. *Eur. J. Biochem.* **1992**, *209*, 895–915.
(22) Van Leeuwen, S. S.; Leeflang, B. R.; Gerwig, G. J.; Kamerling, J. P. *Carbohydr. Res.* **2008**, *343*, 1114–1119.
(23) Kovacik, V.; Bauer, S.; Rosik, J.; Kovac, P. *Carbohydr. Res.* **1968**, *8*, 282–290.
(24) Van der Kaaden, A.; van Doorn-van Wakeren, J. I. M.; Kamerling, J. P.; Vliegenthart, J. F. G.; Tiesjema, R. H. *Eur. J. Biochem.* **1984**, *141*, 513–519.
(25) Veerkamp, J. H.; van Schaik, F. W. *Biochim. Biophys. Acta* **1974**, *348*, 370–387.
(26) Dowd, M. K.; Zeng, J.; French, A. D.; Reilly, P. J. *Carbohydr. Res.* **1992**, *230*, 223–244.

BM800410W